

**A ribosomal protein homolog regulates gene expression and virulence in a bacterial
pathogen**

Hannah S. Trautmann¹ and Kathryn M. Ramsey^{1,2,*}

¹Department of Cell and Molecular Biology, University of Rhode Island, Kingston, RI 02881, USA

²Department of Biomedical and Pharmaceutical Sciences, University of Rhode Island, Kingston, RI
02881, USA

* To whom correspondence should be addressed: Kathryn M. Ramsey kramsey@uri.edu

Abstract

1 The molecular machine necessary for protein synthesis, the ribosome, is generally considered
2 constitutively functioning and lacking any inherent regulatory capacity. Yet ribosomes are commonly
3 heterogenous in composition and the impact of ribosome heterogeneity on translation is not well
4 understood. Here we determine that changes in ribosome protein composition regulate gene
5 expression in the intracellular bacterial pathogen *Francisella tularensis*. *F. tularensis* encodes three
6 distinct homologs for bS21, a ribosomal protein involved in translation initiation, and analysis of
7 purified *F. tularensis* ribosomes reveals they are heterogenous with respect to bS21. Loss of one
8 homolog, bS21-2, results in significant changes to the cellular proteome unlinked to changes in the
9 transcriptome. Among the reduced proteins are components of the type VI secretion system (T6SS), an
10 essential virulence factor encoded by the Francisella Pathogenicity Island. Furthermore, loss of bS21-2
11 leads to an intramacrophage growth defect. Although multiple bS21 homologs complement loss of
12 bS21-2 with respect to T6SS protein abundance, bS21-2 is uniquely necessary for robust
13 intramacrophage growth, suggesting bS21-2 regulates additional virulence gene(s) distinct from the
14 T6SS. Our results indicate that ribosome composition in *F. tularensis*, either directly or indirectly, post-
15 transcriptionally modulates gene expression and virulence. Our findings are consistent with a model in
16 which bS21 homologs function as post-transcriptional regulators, allowing preferential translation of
17 specific subsets of mRNAs, likely at the stage of translation initiation. This work also raises the
18 possibility that bS21 in other organisms may function similarly and that ribosome heterogeneity may
19 permit many bacteria to post-transcriptionally regulate gene expression.

20 **Importance**

21 While bacterial ribosomes are commonly heterogenous in composition (e.g., incorporating
22 different homologs for a ribosomal protein), how heterogeneity impacts translation is unclear. We
23 found that the intracellular human pathogen *Francisella tularensis* has heterogenous ribosomes,
24 incorporating one of three homologs for ribosomal protein bS21. Furthermore, one bS21 homolog
25 post-transcriptionally regulates expression of the *F. tularensis* type VI secretion system, an essential
26 virulence factor. This bS21 homolog is also uniquely important for robust intracellular growth. Our data
27 support a model in which bS21 heterogeneity leads to modulation of translation, providing another
28 source of post-transcriptional gene regulation. Regulation of translation by bS21, or other sources of
29 ribosomal heterogeneity, may be a conserved mechanism to control gene expression across the
30 bacterial phylogeny.

31 Introduction

32 Regulation of translation provides bacteria with a rapid way to modify gene expression. While
33 many distinct mechanisms permit this fine-tuning (1, 2) the impact of ribosome composition on gene
34 expression remains poorly-understood. In bacteria, ribosomes are diverse and commonly
35 heterogenous with respect to ribosomal protein (r-protein) content, post-translational modifications,
36 rRNA content, or post-transcriptional modifications (reviewed in 3). The functional consequences of
37 ribosome heterogeneity are unclear but may include the formation of “specialized ribosomes,” or
38 ribosomes with altered activity due to their distinct composition (4). Although specialized ribosomes
39 are not well described in bacteria, exciting recent studies have connected altered rRNA content of
40 ribosomes and gene regulation (5, 6) and, in *Mycobacterium smegmatis*, ribosomes containing
41 alternate r-protein homologs translate some genes with differential efficiency (7).

42 *Francisella tularensis* is a Gram-negative, facultative intracellular bacterium that causes the
43 potentially fatal human disease tularemia (8). After internalization into host cells, *F. tularensis* must
44 escape from the Francisella-containing phagosome to replicate inside the cytosol. This escape process
45 requires a type VI secretion system (T6SS), which modifies the host cell by delivery of effector proteins
46 (9–12). Production of this T6SS is coordinately regulated by the transcription factors MglA, SspA, and
47 PigR, as well as the signaling molecule ppGpp (13–20). Regulation of the T6SS is arguably the most
48 well-understood virulence regulatory network in *F. tularensis*. However, much remains to be learned
49 about the regulation of other virulence factors.

50 Despite its relatively small genome (< 2 Mbp), *F. tularensis* encodes three distinct *rpsU* genes
51 (*rpsU1*, *rpsU2*, and *rpsU3*), which encode homologs of the small ribosomal subunit protein bS21 (bS21-
52 1, bS21-2, and bS21-3, respectively). This is the only apparent source of ribosome heterogeneity in *F.*

53 *tularensis*, as the three rRNA operon sequences are identical and no other r-proteins are encoded by
54 multiple homologs. In *Escherichia coli*, bS21 is involved in translation initiation (21, 22) and, consistent
55 with this activity, is found on the ribosome close to the anti-Shine-Dalgarno sequence near the mRNA
56 exit channel (23, 24). Furthermore, bS21 is one of the last r-proteins to assemble into the ribosome, is
57 considered “loosely associated,” and is easily exchanged among assembled ribosomes (25, 26).

58 Using mass spectrometry and immunoblot analyses, we show that ribosomes in *F. tularensis* are
59 heterogenous with respect to bS21 content and can incorporate any of the three bS21 homologs into
60 actively-translating ribosomes. Using quantitative whole-cell proteomics, quantitative immunoblots,
61 and transcriptomic analyses, we demonstrate that loss of a particular bS21 homolog, bS21-2, leads to
62 changes in abundance for a subset of proteins that cannot be explained by changes in transcript
63 abundance. Among the regulated proteins are multiple virulence factors, including those that comprise
64 the T6SS. Finally, using intramacrophage growth assays, we provide evidence that bS21-2, and not the
65 other bS21 homologs, promotes intramacrophage growth. Our findings reveal that a specific r-protein
66 homolog in *F. tularensis*, bS21-2, regulates gene expression at the level of protein abundance and is a
67 positive regulator of virulence.

68

69 **Results**

70 ***Francisella* species encode three bS21 homologs**

71 The genomes of multiple *Francisella* species contain three distinct genes encoding bS21 (*rpsU1*,
72 *rpsU2*, and *rpsU3*), raising the possibility that cells contain ribosomes that are heterogenous with
73 respect to bS21 content. The gene encoding one homolog in *F. tularensis*, *rpsU2* (encoding bS21-2), is

74 syntenic with the single bS21-encoding gene in *Escherichia coli* (**Figure S1**). In *E. coli*, *rpsU* is the first in
75 an operon referred to as the macromolecular synthesis operon, encoding key proteins for initiation of
76 translation (bS21), DNA replication (DNA primase), and transcription (RNA polymerase σ^{70}) (27). The
77 corresponding operon in *Francisella* species including *F. tularensis* also contains *yqeY*, which may
78 encode a protein necessary for correct tRNA aminoacylation (28). Another bS21 homolog, bS21-1, is
79 encoded by *rpsU1* in an apparent operon downstream of the gene for cold shock protein CspC. There
80 are no annotated genes in the same transcriptional context as *rpsU3*, the gene encoding the third
81 homolog, bS21-3. The bS21 homologs in *F. tularensis* are distinct but similar, with amino acid identities
82 ranging from 48 – 72%, and are similar to *E. coli* bS21 (51 – 60% identical, with bS21-2 having the
83 highest identity; **Figure S2**).

84 ***F. tularensis* ribosomes are heterogenous**

85 The presence of three distinct genes encoding bS21 raises the potential for *F. tularensis*
86 ribosomes to be heterogenous with respect to bS21. To investigate this possibility, we used sucrose
87 cushion centrifugation to isolate ribosomes from *F. tularensis* LVS grown *in vitro* in quadruplicate and
88 analyzed their protein composition using liquid chromatography tandem mass spectrometry (LC-
89 MS/MS). Approximately 80% of the spectral counts corresponded to ribosomal proteins or proteins
90 associated with transcription and translation complexes (e.g., RNA polymerase, translation release
91 factors, SRP), indicating *F. tularensis* ribosomes purified in this manner are highly pure (**Figure 1A**,
92 **Table S1**). Despite the small size of bS21 (approx. 8 kDa), we identified multiple peptides corresponding
93 to bS21-2 in all samples. In one sample, peptides shared between bS21-1 and bS21-3 were detected
94 (**Figure 1B**). This suggests that bS21-2 is the most abundant homolog in wild-type cells, consistent with

95 its production from an operon encoding proteins essential for transcription and DNA replication. It also
96 suggests that either bS21-1, bS21-3, or both, are incorporated into ribosomes in LVS. However, it does
97 not allow us to determine the next-most abundant homolog (bS21-1 or bS21-3) or confirm
98 incorporation of both of these other homologs. Regardless, these results demonstrate that multiple
99 bS21 homologs are incorporated into wild-type *F. tularensis* ribosomes and that ribosomes in *F.*
100 *tularensis* are heterogenous, containing different bS21 homologs.

101 We next wanted to determine if each bS21 homolog can be found in actively-translating
102 ribosomes. To track each bS21, we modified each homolog to encode a C-terminal vesicular stomatitis
103 virus glycoprotein (VSV-G) tag and ectopically expressed them individually from a plasmid , using the
104 same promoter, in wild-type cells. Lysate fractions of these cells were analyzed by immunoblotting
105 after sucrose gradient sedimentation (**Figure 1C; Figure S3**). When ectopically expressed (rather than
106 produced from its native locus), bS21-1 was the least abundant homolog while bS21-3 was produced at
107 the highest level. Each homolog was found in fractions corresponding to the 30S, 70S, and polysomes.
108 Although bS21 is thought to function primarily in translation initiation, our findings indicate that each
109 bS21 homolog associates with the ribosome throughout the translation cycle.

110 ***Loss of bS21-2 leads to changes in protein, not transcript, abundance***

111 Because the ribosomal protein bS21 is involved in translation initiation, we hypothesized that
112 loss of a bS21 homolog may impact translation and result in changes in abundance in a subset of
113 proteins. To test this hypothesis, we individually deleted each of the three genes encoding bS21
114 homologs. This led us to determine that no single bS21 homolog is essential for cell growth. We
115 subsequently grew wild-type cells and cells lacking single bS21 homologs to mid-log *in vitro* and used

116 data-independent acquisition (DIA) mass spectrometry analysis (29) to compare relative protein
117 abundance in cell lysates. Using this method, 68% of the total proteins predicted to be encoded by *F.*
118 *tularensis* LVS were identified and analyzed (1194 of 1754). When compared to wild-type, we did not
119 detect any significant changes in protein abundance in cells lacking either of the two lower-abundance
120 bS21 homologs, bS21-1 and bS21-3 (>1.5-fold altered with an adjusted p-value <0.05, excluding bS21).
121 In contrast, cells lacking the most abundant homolog, bS21-2 ($\Delta rpsU2$), had significant proteomic
122 differences compared to wild-type cells. Specifically, we found 185 unique proteins (~16% of detected
123 proteins) have altered abundance in cells without bS21-2 compared to wild-type cells (**Figure 2**, data
124 on y-axis, **Table S2**).

125 To determine if these changes in protein abundance can be explained by corresponding
126 changes in transcription, we performed transcriptomic analyses on wild-type cells, cells lacking bS21-2
127 ($\Delta rpsU2$), and cells lacking the native bS21-2 but ectopically expressing bS21-2-V from a plasmid.
128 Comparing cells with and without native bS21-2, we identified 105 differentially expressed genes (>2-
129 fold altered with an adjusted p-value <0.05, excluding *rpsU*; **Figure 2**, data on x-axis, **Table S3**). All of
130 these changes were complemented by ectopic expression of bS21-2-V on a plasmid.

131 Our analysis revealed that in cells lacking bS21-2, the largest change in transcript abundance is
132 a six-fold increase in *yqeY*, the gene directly downstream from *rpsU2* (which encodes bS21-2). This
133 increase in transcript abundance is complemented by ectopic expression of bS21-2-V, suggesting that
134 bS21-2 functions as a negative regulator of its own operon. Translational feedback regulation is well-
135 established for multiple ribosomal proteins but, to the best of our knowledge, this is the first report of

136 translational regulation of ribosomal proteins in *F. tularensis* and the first report that bS21 regulates its
137 own production (30, 31).

138 Comparison of our proteomic and transcriptomic analyses reveals that the changes in protein
139 abundance are not generally due to changes in transcript abundance. Of the 185 differentially
140 abundant proteins in cells lacking bS21-2, only ~12% (23) can be explained by altered transcription
141 (**Figure 2**, yellow dots), while about 88% (162; **Figure 2**, blue dots and orange dot) have changes in
142 protein abundance without a corresponding change in transcript abundance. These discrepancies
143 between transcript abundance and protein abundance support a model in which bS21-2 controls
144 expression, either directly or indirectly, of some genes at the level of translation.

145 ***bS21-2 controls the abundance of type VI secretion system proteins, which are essential for virulence***

146 Among the proteins with altered abundance in cells lacking bS21-2, we identified twelve out of
147 sixteen proteins encoded on the Francisella pathogenicity island (FPI). The FPI encodes a unique type VI
148 secretion system (T6SS) that is absolutely essential for intramacrophage growth and virulence of
149 *F. tularensis* (32–34). Using quantitative immunoblotting and antibodies specific to a subset of
150 *F. tularensis* T6SS proteins, we validated that cells lacking bS21-2 have differences in those T6SS
151 proteins (**Figure 3**). Consistent with the mass spectrometry results, we found reductions in virtually all
152 probed T6SS proteins, including an ~4-fold reduction in PdpB, the TssM/IcmF homolog. Using this
153 approach, we also found an ~2.4-fold reduction in IgIA and ~1.7-fold reduction in IgIB, T6SS proteins
154 that are just below the cutoff for statistical significance in our mass spectrometry analysis. Since we
155 identified this differential abundance using a more sensitive method of comparison, it raises the
156 possibility that all FPI-encoded proteins may be differentially abundant in cells lacking bS21-2

157 compared to wild-type cells, but we do not have antibodies specific to the remaining proteins (i.e.,
158 PdpE and VgrG) to test this hypothesis. Also consistent with our mass spectrometry findings, IgID (the
159 homolog of TssK) is the only T6SS protein with increased, rather than decreased, protein abundance
160 (**Figure 3**). Each of these changes in protein abundance can be complemented by ectopic expression of
161 bS21-2-V, driven by the *groES* promoter on a plasmid (**Figure 3**).

162 These changes in protein abundance likely reflect positive regulation of most, but not all, T6SS
163 proteins by bS21-2 at the level of translation, either directly or indirectly. Our findings are inconsistent
164 with bS21 positively regulating transcription; it is well-established that transcription of FPI operons are
165 coordinately controlled and our RNA-Seq analysis reveals that cells lacking bS21-2 do not have FPI-wide
166 transcript reductions (**Table S4**) (13–16, 20, 35). In a complementary approach, we compared the
167 transcript abundance for specific FPI genes using quantitative RT-PCR and included cells lacking PigR, a
168 transcription factor critical for positive transcriptional regulation of FPI genes (14–16, 20, 35)(**Figure**
169 **S4**). We confirmed that cells lacking PigR have major decreases in FPI transcript abundance but cells
170 lacking bS21-2 do not have compelling (2-fold or greater) changes in FPI transcript abundance or in
171 transcript abundance of the positive regulator PigR, consistent with the RNA-Seq results. We
172 considered the possibility that loss of bS21-2 could indirectly impact T6SS protein abundance by
173 altering protein stability, but the half-life of one of the most differentially regulated proteins, PdpB,
174 was unchanged in cells with and without bS21-2 (longer than 120 minutes, **Figure S5**). Our results are
175 consistent with bS21-2 controlling expression of T6SS proteins at the level of translation.

176 ***Other bS21 homologs impact the abundance of type VI secretion system proteins***

177 Our findings indicate that bS21-2 is the most abundant bS21 homolog in wild-type cells of LVS.
178 However, it is not clear if the majority of ribosomes in cells lacking bS21-2 incorporate another bS21
179 homolog or no bS21 at all. This leads to the question: do all bS21 homologs regulate T6SS protein
180 translation or does bS21-2 specifically control translation of T6SS proteins? To answer this question, we
181 ectopically expressed either bS21-1-V or bS21-3-V in cells lacking bS21-2, similarly to the ectopic
182 expression of bS21-2-V. We subsequently used quantitative immunoblot analyses to assess the
183 abundance of each ectopically expressed bS21 homolog and a subset of T6SS proteins (**Figure 3**). While
184 this strategy resulted in comparable amounts of bS21-2 and bS21-3, ectopic expression results in
185 approximately 2-fold less bS21-1 than the other homologs, consistent with its lower expression in wild-
186 type cells (**Figure 3, Figure 1**). With respect to T6SS protein abundance, ectopic expression of bS21-3
187 restores all probed proteins to wild-type levels, complementing the loss of bS21-2 (**Figure 3**). However,
188 bS21-1 does not appear to complement T6SS protein production completely (**Figure 3**). This may be
189 due to reduced levels of bS21-1, lack of specific ability to regulate of T6SS proteins, or a combination of
190 the two factors. Notably, loss of bS21-2 results in a growth defect (**Table S5**) that can be
191 complemented by ectopic expression of bS21-2 or bS21-1, but not bS21-3. That cells lacking bS21-2
192 with ectopic expression of bS21-3 have wild-type levels of T6SS proteins and yet still have a growth
193 defect reveals that changes in T6SS proteins are not due simply to changes in growth rate. Our findings
194 allow us to conclude that incorporation of either bS21-2 or bS21-3 – and to a lesser extent, bS21-1 –
195 into ribosomes regulates production of T6SS proteins.

196 ***bS21-2 is important for intramacrophage growth***

197 A functional T6SS is essential for *F. tularensis* intramacrophage replication and is a strict
198 requirement for virulence (32–34). The observed differences in FPI protein abundance led us to
199 hypothesize that T6SS function may be compromised in cells lacking bS21-2 and these cells may be
200 attenuated for intramacrophage growth. We tested the ability of cells lacking bS21-2 ($\Delta rpsU2$) to
201 survive in murine macrophage-like J774A.1 cells. This revealed a significant defect in the ability of
202 bS21-2 mutant cells to replicate in macrophage; we recovered ten-fold fewer bS21-2 mutant bacteria
203 after 24 hours compared to wild-type (**Figure 4**). The intramacrophage growth defect of cells lacking
204 bS21-2 can be restored by ectopic expression of bS21-2 from a plasmid (**Figure 4**). This is in contrast to
205 ectopic expression of bS21-1 and bS21-3, neither of which restores the intramacrophage growth of
206 cells lacking bS21-2 (**Figure 4**). These results indicate that bS21-2 is specifically required for
207 intramacrophage survival, despite the fact that ectopic expression of bS21-1 restores *in vitro* growth
208 rates and ectopic expression of bS21-3 restores T6SS protein production *in vitro* (**Figure 3, Table S5**).

209 In summary, only the presence of bS21-2, not bS21-1 or bS21-3, can restore the
210 intramacrophage growth defect of cells without bS21-2. This reveals that bS21-2 is critical for *F.*
211 *tularensis* virulence and fits a model in which bS21-2 specifically regulates one or more genes
212 necessary for intramacrophage growth in addition to T6SS genes, a topic still under investigation.

213 Discussion

214 The findings described here reveal that ribosome composition in *F. tularensis* is heterogenous
215 with respect to the small ribosomal protein bS21 and that this heterogeneity impacts regulation of
216 gene expression at the level of translation. In particular, by studying cells that contain ribosomes either
217 with or without one of the three bS21 homologs, we have identified bS21-2 as a positive regulator of

218 most of the T6SS proteins. Additionally, cells lacking bS21-2 are defective for intramacrophage growth;
219 since this defect can only be complemented by bS21-2, even though bS21-3 and (to a lesser extent)
220 bS21-1 can restore T6SS protein abundance, this intramacrophage growth defect may be independent
221 of the impact bS21-2 has on the T6SS. This allows us to conclude that bS21-2 is important for the
222 intramacrophage growth of *F. tularensis*, potentially by regulating the translation of one or more
223 proteins (in addition to the T6SS), necessary for virulence.

224 Our approach in studying bS21 homologs in *F. tularensis* has thus far focused on the homolog
225 bS21-2, whose loss led to phenotypic change. Our data suggest that bS21-2 is the most abundant
226 homolog in the conditions studied. We hypothesize that cells without bS21-1 and bS21-3 did not
227 exhibit distinct phenotypes under the conditions of our experiments due to their relatively low
228 abundance. Both of these homologs may also regulate gene expression under conditions when they
229 are more abundant, but these conditions are not yet identified. Additionally, in our study of cells
230 without bS21-2, it is not clear if the majority of ribosomes lack bS21 entirely or instead incorporate
231 bS21-1 or bS21-3; our findings only extend to heterogeneity with respect to the presence or absence of
232 bS21-2.

233 Comparison of *rpsU* genes across the bacterial phylogeny reveals that many clades and species
234 do not encode bS21, suggesting that it is not essential for translation (36, 37). However, targeted
235 deletion of the single *rpsU* gene in *E. coli* has not been successful, suggesting bS21 is essential in *E. coli*
236 (38–40). We reported in previous work that the *F. tularensis* homolog syntenic with *E. coli* *rpsU*, *rpsU2*,
237 is essential *in vitro* using transposon-insertion sequencing (Tn-Seq) (41). Yet using a targeted allelic
238 exchange approach, we have been able to successfully delete each *rpsU* homolog individually,

239 indicating that none of the bS21 homologs is individually essential. Our identification of *rpsU2* as an
240 essential gene was likely due to the polar effects of transposon insertion into the first gene of an
241 operon containing other known essential genes (*dnaG*, encoding primase, and *rpoD*, encoding the σ^{70}
242 subunit of RNA polymerase). It is unclear if *F. tularensis* cells lacking all three *rpsU* genes are viable.

243 The literature reflects that bS21 may regulate gene expression in other bacteria. A recent study
244 of the *Flavobacterium johnsoniae* ribosome revealed that bS21 plays a role in sequestering the anti-
245 Shine-Dalgarno sequence (42). This occlusion occurs through contacts with the C-terminal region of
246 bS21 that are conserved across Bacteroidetes species and provides a rationale to explain why most
247 Bacteroidetes mRNAs lack Shine-Dalgarno sequences. Notably, the mRNA encoding bS21 in *F.*
248 *johnsoniae* encodes a perfect Shine-Dalgarno sequence, strongly suggesting that bS21 regulates its
249 own expression through translational autoregulation (42). *F. tularensis*, however, is a member of the
250 Gammaproteobacteria, has bS21 homologs that exhibit significant differences from *F. johnsoniae* at
251 the C-terminal region, and encodes mRNAs that commonly contain sequences similar to the consensus
252 Shine-Dalgarno sequence. This suggests that in *F. tularensis*, bS21 exerts its effects on gene expression
253 in a different manner.

254 In other bacteria that encode it, loss of bS21 leads to a variety of phenotypic changes. In *B.*
255 *subtilis*, loss of bS21 results in biofilm and motility defects (43) and in *Listeria monocytogenes*,
256 inactivation of bS21 is linked to stress resistance and altered transcript abundance(44, 45).
257 *Staphylococcus aureus* lacking functional bS21 exhibit increased resistance to the antibiotics
258 daptomycin and vancomycin (46–48). Both *Burkholderia pseudomallei* and *F. tularensis* encode
259 multiple bS21 homologs and in both organisms, virulence screens using transposon mutagenesis have

260 identified one homolog as important for virulence (49, 50). Together, these findings suggest that bS21
261 may regulate gene expression in diverse bacterial species.

262 The idea that bS21 might modulate translation for a subset of mRNAs is further supported by
263 the recent discovery that bS21 is encoded by thousands of sequenced bacteriophage genomes and is
264 one of the most commonly encoded phage ribosomal proteins (51, 52). Transcripts encoding bS21 have
265 been detected in metatranscriptomic samples along with transcripts for late-stage replication proteins
266 (53) and at least one phage-encoded bS21 can be incorporated into *E. coli* ribosomes (51). All of this
267 raises the possibility that incorporation of a viral bS21 into the host ribosome may co-opt the
268 translation machinery in favor of viral proteins and replication.

269 Our work, together with these earlier findings, strongly suggests that incorporation of bS21 into
270 the ribosome can impact translation of a subset of mRNAs. Considering that bS21 can easily be
271 exchanged among ribosomes, this provides an excellent mechanism to quickly fine-tune the cellular
272 proteome. While the molecular mechanism leading to the modulation of translation has yet to be
273 identified, it is reasonable to speculate that bS21 impacts translation during initiation through specific
274 interactions with the 5' untranslated regions of a specific set of mRNAs. These findings also support the
275 idea that changes in ribosome composition may impact translation and provide another source for
276 bacterial control of gene expression.

277

278 **Materials and Methods**

279 ***Bacterial strains and growth conditions***

280 Unless otherwise noted, bacterial strains were grown as indicated here. *Francisella tularensis* subsp.
281 *Holarctica* Live Vaccine Strain (LVS) cells were grown in Mueller-Hinton broth (BD Difco) supplemented
282 with 0.025% iron pyrophosphate, 0.1% glucose, and 2% Isovitalex (sMHB), shaking aerobically or on
283 cystine heart agar plates with 1% hemoglobin (CHA-H) at 37°C. *Escherichia coli* XL1-Blue cells were
284 grown in lysogeny broth (LB) shaking aerobically or on LB agar plates at 37°C. Kanamycin was used at
285 concentrations of 5 µg/mL (*F. tularensis*) or 50 µg/mL (*E. coli*).

286

287 ***Vector construction***

288 Complementation plasmids for each bS21 homolog were created from a plasmid derived from
289 pFNLT6 (54), pKL42 (pF-PmrA-V). Specifically, the complementation plasmids produce bS21 homologs
290 with a C-terminal VSV-G epitope under the control of the *F. tularensis* *groES* promoter. Each *rpsU* gene
291 was amplified using a 5' primer specifying an EcoRI site and an ideal Shine-Dalgarno sequence (5'-
292 AGGAGG-3') located six nucleotides upstream from the translation start site. The 3' primer did not
293 include the native stop codon and included DNA specifying a NotI site. The fragment was cloned into
294 EcoRI/NotI digested pKL42, such that the 3' end of each *rpsU* is in frame with codons specifying three
295 alanines followed by the VSV-G epitope. The resulting plasmids were pKR6 pF-bS21-1-V, pKR7 pF-bS21-
296 2-V, and pKR8 pF-bS21-3-V. The control plasmid pF is the original pFNLT6 plasmid (containing the
297 *groES* promoter but not any *rpsU* genes nor the VSV-G epitope).

298

299 The plasmid pEX18kan was modified to generate in-frame deletions of each *rpsU* gene as previously
300 described (14). Flanking regions of ~600 base pairs from both sides of each *rpsU* gene were amplified

301 by PCR. Primers amplifying the DNA adjacent to each *rpsU* gene included the first three or last three
302 codons of the open reading frame and DNA specifying a NotI site, which also encodes an alanine linker
303 (5'-GCGGCCGCT-3'). The two fragments were cloned into BamHI/KpnI-digested pEX18kan for each
304 *rpsU* gene respectively, yielding pKL122 pEXΔ*rpsU1*, pKR11 pEXΔ*rpsU2*, and pKR12 pEXΔ*rpsU3*; these
305 plasmids were used to construct deletions via allelic exchange as described below.

306

307 ***Strain construction***

308 Deletion strains were constructed by allelic exchange as previously (55). Briefly, competent cells were
309 made by washing *F. tularensis* LVS cells in 10% sucrose and resuspending in an equal volume of 10%
310 sucrose to cells. At least 1 μg of allelic exchange plasmid was electroporated into 50 μL competent cells
311 in 0.2 cm cuvettes with a 2.5 kV pulse. Cells were allowed to recover in 4 – 5 mL sMHB for 4-8 hours at
312 37°C, shaking. Cells in which a single integration event occurred were selected for on CHA-H plates
313 with kanamycin. These cells were subsequently plated on CHA-H containing 10% sucrose and lacking
314 NaCl, allowing for survival only of cells that had crossed out the non-homologous portion of the vector,
315 including *sacB* and kanamycin resistance gene. Colonies that were sucrose-resistant and kanamycin-
316 sensitive were screened for deletions using PCR. Candidate strains were confirmed by amplification of
317 genomic DNA outside of the flanking regions on each side of the deletion and Sanger sequencing
318 (Rhode Island Genomics and Sequencing Center). Plasmid pKL122 pEXΔ*rpsU1* was used to make LVS
319 Δ*rpsU1*, plasmid pRK11 pEXΔ*rpsU2* was used to make LVS Δ*rpsU2*, and plasmid pKR12 pEXΔ*rpsU3* was
320 used to make LVS Δ*rpsU3*.

321

322 Complementation plasmids were electroporated into LVS or LVS *ΔrpsU2* cells as described above and
323 selected for on CHA-H plates with kanamycin.

324

325 ***Immunoblotting***

326 Cells were collected from mid-log cultures (OD₆₀₀ 0.3-0.4) and resuspended in sample loading buffer
327 (SLB: 1X NuPAGE LDS with 50 mM DTT) normalized to OD₆₀₀ and heated at 95°C for 10 minutes. Cell
328 lysates and fractions were separated by SDS-PAGE on 4-12% Bis-Tris NuPAGE gels in MES or MOPS
329 running buffer (Invitrogen) and transferred to PVDF with the Mini Blot Module transfer system
330 (Invitrogen; 20V for 1 hour on ice) or the Criterion cell for midi gels (BioRad; 60V for 40 minutes on ice)
331 with 1X NuPAGE transfer buffer and 10% methanol. Whole cell lysates were analyzed for total protein
332 with the Invitrogen No-Stain Protein labeling reagent and all membranes were blocked with Odyssey
333 blocking buffer diluted 1:5 in PBS overnight. For each antibody, the linear range of protein detection
334 was determined by plotting sequential dilutions of one lysate from each strain as a standard curve to
335 establish appropriate volume of lysate to load. Membranes were probed with indicated monoclonal
336 antibodies (BEI Resources, diluted 1:1000 in blocking buffer for all antibodies except anti-PdpB, which
337 was diluted 1:250) or the VSV-G epitope (Sigma, diluted 1:2222). Proteins were detected using IRDye
338 800 CW donkey anti-mouse IgG or donkey anti-rabbit IgG (Li-Cor, diluted 1:10,000). Fluorescence was
339 measured and quantified on the LiCor Odyssey CLx imager and software, and protein abundance was
340 calculated relative to total protein in each lane. Experiments were performed at least twice in
341 biological triplicate and two to three technical replicates.

342

343 **RNA isolation and qRT-PCR**

344 Cells were collected from mid-log cultures (OD₆₀₀ 0.3-0.4). Nucleic acids were isolated using the Direct-
345 Zol RNA purification kit (Zymo Research) according to the manufacturer's protocol. Purified nucleic
346 acids were treated with RQ1 Dnase (Promega) for 1 hour at 37°C and RNA was purified with the Direct-
347 Zol RNA purification kit. cDNA was synthesized using Superscript III reverse transcriptase (Life
348 Technologies) as previously described (14). qRT-PCR was performed using PowerUp SYBR Green
349 Master Mix (Applied Biosystems) and a Roche LightCycler 480 (University of Rhode Island Genomics
350 and Sequencing Center) essentially as described (14). Transcript abundances of *pdpA*, *pdpB*, *iglA*, and
351 *pigR* were compared to three different control genes (*tul4*, *rpoA1*, and *bfr*) and since all results were
352 similar, relative abundance is reported to *tul4*. Experiments comparing wild-type and *rpsU2* mutant
353 cells were performed three times in biological triplicate; experiment with cells lacking PigR was
354 performed once.

355

356 **RNA-Seq**

357 Approximately 1.5 µg of RNA isolated as above was sent to the Microbial Genome Sequencing Center
358 (MiGS) for RNA-Seq analysis, in biological triplicate (LVS pF) or duplicate (LVS $\Delta rpsU2$ pF, LVS $\Delta rpsU2$
359 pF-bS21-2-V). After using RiboZero Plus rRNA depletion, libraries were made using Illumina Stranded
360 RNA library preparation and sequenced for a minimum of 12 million paired end reads. Sequencing
361 reads will be available in the National Center for Biotechnology Information Gene Expression Omnibus
362 (GEO). Paired-end sequencing reads were mapped to the *F. tularensis* LVS genome (NCBI RefSeq
363 accession number NC_007880) using bowtie2 version 2.2.4. Reads that mapped to annotated genes
364 were counted using HTSeq version 0.11.2, and analysis of differential gene expression was conducted

365 using DESeq2 version 1.32.0. Reported genes had a 2-fold-higher or -lower abundance than the wild
366 type, all with an adjusted p-value of 0.05 or lower.

367

368 ***70S ribosome purification***

369 70S ribosomes were isolated using sucrose cushion centrifugation essentially as described (56). Briefly,
370 wild-type *F. tularensis* cells were grown in 500 mL sMHB to mid-log (OD₆₀₀ 0.3-0.4). Cells were chilled
371 on ice for 20 minutes, centrifuged at 11,000 x g for 5 minutes at 4°C, then washed once with buffer
372 H¹⁰M¹⁰A¹⁰⁰⁰ (10 mM HEPES KOH pH 7.6, 10 mM MgCl₂, and 100 mM NH₄Cl) to remove ribonucleases.
373 The pellet was then washed twice with buffer H¹⁰M¹⁰A⁵⁰ (10 mM HEPES KOH pH 7.6, 10 mM MgCl₂, and
374 50 mM NH₄Cl, with or without 5 mM β-mercaptoethanol [BME]), and resuspended in ~15 mL of
375 H¹⁰M¹⁰A⁵⁰ with 20 U Dnase I. Cells were lysed by passing through a French press three times at 800 psi
376 and cell debris were removed by centrifugation at 146,000 x g for 15 minutes at 4°C. Supernatant was
377 incubated with 0.5% Brij58 for 30 minutes and layered on top of H¹⁰M¹⁰A⁵⁰⁰ + 20% sucrose (10 mM
378 HEPES KOH pH 7.6, 10 mM MgCl₂, 500 mM NH₄Cl, 20% sucrose, with or without 5 mM BME).
379 Ribosomes were pelleted by ultracentrifugation in 70 Ti rotor for 4 hours at 146,000 x g at 4°C. The
380 pellet was washed twice with H¹⁰M¹⁰A⁵⁰ and gently resuspended in H¹⁰M¹⁰A⁵⁰. This suspension was
381 then layered onto another sucrose cushion (H¹⁰M¹⁰A⁵⁰ with 40% sucrose) and centrifuged for 14 hours
382 at 146,000 x g at 4°C to further purify the ribosomes. Purified 70S ribosomes were gently resuspended
383 in ~250 μL of H¹⁰M¹⁰A⁵⁰ and stored at -80°C.

384

385 ***LC-MS/MS of purified LVS ribosomes***

386 70S ribosomes from wild-type LVS cells were prepared as described above. Samples were either
387 purified via gel stacking prior to mass spectrometry analysis or maintained in H¹⁰M¹⁰A⁵⁰ and delivered
388 to the Northwestern Proteomics Core. The proteins were in-gel digested or in-solution digested and
389 liquid chromatography tandem mass spectrometry (LC-MS/MS) analysis was completed based on
390 internal protocols, matching peptides to the *F. tularensis* LVS proteome (NC_007880).

391

392 ***DIA mass spectrometry***

393 Cells were collected from mid-log cultures (OD₆₀₀ 0.3-0.4) and resuspended in Buffer 1 (20 mM KHEPES
394 pH 7.9, 50 mM KCl, 0.5 mM DTT) with protease inhibitor tablets (Complete Mini, EDTA-free, Roche).
395 Cells were lysed by sonication and protein concentration was determined using a BCA protein assay
396 (Pierce). Lysates with concentrations between 620 and 862 µg/mL were used by the University of
397 Arkansas for Medical Sciences (UAMS) Proteomics Core for analysis. Protein extraction and protease
398 digestion was completed according to UAMS internal protocols. Data-independent acquisition (DIA)
399 was completed with the Orbitrap Exploris 480 mass spectrometer.

400

401 ***Polysome purification and sucrose gradient sedimentation***

402 Polysomes were isolated essentially as described (57). *F. tularensis* cells were grown until early log
403 (OD₆₀₀ 0.2-0.25). Liquid cultures were rapidly filtered through 0.2 µm nitrocellulose membranes and
404 transferred to a conical tube filled with liquid nitrogen. Cells were lysed by bead-beating with 650 µL
405 flash frozen lysis buffer (25 mM HEPES pH 7.6, 100 mM NH₄Cl, 10 mM MgCl₂, 0.4% Triton X-100, 0.1%

NP-40, 100 U/mL Rnase-free Dnase) using the TissueLyser II (Qiagen) five times (15 Hz, 3 mins). Cell debris was pelleted and the polysome-containing lysates were stored at -80°C.

Sucrose gradients were prepared using 10 and 55% sucrose solutions in 25 mM HEPES pH 7.6, 100 mM NH₄Cl, 10 mM MgCl₂ with the BioComp Instruments 153 Gradient Station (BioComp). Cell lysates were layered onto gradients and centrifuged with the Beckman-Coulter SW40 Ti rotor at 40,000 rpm for 2.5 hr at 4°C. Gradients were fractionated using the Triax full spectrum flow cell and fractionator (BioComp; 0.2 mm/s, 28 fractions) and A260 was measured every second. Collected fractions were stored at -80°C. 20 µL of each fraction was combined with 10 µL of sample loading buffer (3X NuPAGE LDS with 50 mM DTT) and immunoblotted as described above.

416

417 ***Intramacrophage replication assays***

Intramacrophage growth assays were performed as previously described (55). Briefly, approximately 2.5 x 10⁴ cells of murine macrophage-like J774A.1 cells were incubated at 37°C in 5% CO₂ overnight in 96-well plates in DMEM (Invitrogen) supplemented with 10% fetal bovine serum (Gemini Bio-Products; DMEM-F). Macrophage cells were infected with LVS and indicated derivative strains at an MOI of approximately 5 – 10. After two hours, cells were washed twice with PBS and media was replaced with DMEM-F containing 10 µg/mL gentamycin. After 2 or 24 hours of infection, macrophage were lysed for 30 minutes in 1% saponin in PBS and plated for enumeration.

425

426 ***Antibiotic chase experiment***

427 Indicated *F. tularensis* LVS cells were grown to mid-log in liquid culture (OD₆₀₀ 0.3-0.4). Spectinomycin
428 was added to a final concentration of 200 µg/mL. Cells were collected at the indicated time points after
429 antibiotic addition and resuspended in sample loading buffer normalized to OD₆₀₀ at t=0.
430 Immunoblotting was conducted as described above and analysis was conducted using one-phase decay
431 equation on Prism 9 (GraphPad). Data represents two experiments in biological triplicate.

432

433 ***Acknowledgements***

434 For helpful comments on the manuscript, we thank Dr. Simon L. Dove, Dr. Steven T. Gregory, and Dr.
435 Matthew M. Ramsey. For use of shared equipment, we thank Dr. Gregory, Dr. Jodi L. Camberg, and Dr.
436 Niall G. Howlett. We thank the other members of the Ramsey laboratory. We also thank Janet Atoyan
437 and the URI Genomics and Sequencing Center (now Rhode Island INBRE Molecular Informatics Core).

438

439 ***Funding Information***

440 This work was funded by a NIGMS CARTD-COBRE Pilot Project Award (P20GM121344—KMR), a
441 NIGMS/RI-INBRE Early Career Development Award (P20GM103430—KMR), and a Rhode Island
442 Foundation Medical Research Grant (2798_20190602—KMR). This work was supported by the USDA
443 National Institute of Food and Agriculture, Hatch Formula project accession number 1017848.

444

445 This material is based upon work conducted at a Rhode Island NSF EPSCoR research facility, the
446 Genomics and Sequencing Center, supported in part by the National Science Foundation EPSCoR
447 Cooperative Agreements 0554548, EPS-1004057, and OIA-1655221. Research was made possible by
448 the use of equipment and services available through the Rhode Island Institutional Development

449 Award (IDeA) Network of Biomedical Research Excellence from the National Institute of General
450 Medical Sciences of the National Institutes of Health under grant number P20GM103430 through the
451 Centralized Research Core facility and the Molecular Informatics Core (RRID:SCR_017685). LC-MS/MS
452 proteomics were performed by the Northwestern Proteomics Core Facility, supported by NCI CCSG P30
453 CA060553, instrumentation award (S10OD025194), and the National Resource for Translational and
454 Developmental Proteomics supported by P41 GM108569. DIA proteomics were performed by IDeA
455 National Resource for Quantitative Proteomics, supported by NIGMS R24GM137786.

456

457 **References**

458

- 459 1. Hershey JWB, Sonenberg N, Mathews MB. 2012. Principles of Translational Control: An Overview.
460 Cold Spring Harb Perspect Biol 4:a011528.
- 461 2. Duval M, Simonetti A, Caldelari I, Marzi S. 2015. Multiple ways to regulate translation initiation in
462 bacteria: Mechanisms, regulatory circuits, dynamics. Biochimie 114:18–29.
- 463 3. Byrgazov K, Vesper O, Moll I. 2013. Ribosome heterogeneity: another level of complexity in bacterial
464 translation regulation. Curr Opin Microbiol 16:133–139.
- 465 4. Xue S, Barna M. 2012. Specialized ribosomes: a new frontier in gene regulation and organismal
466 biology. Nat Rev Mol Cell Bio 13:355–69.
- 467 5. Kurylo CM, Parks MM, Juetten MF, Zinshteyn B, Altman RB, Thibado JK, Vincent CT, Blanchard SC.
468 2018. Endogenous rRNA Sequence Variation Can Regulate Stress Response Gene Expression and
469 Phenotype. Cell Rep 25:236-248.e6.
- 470 6. Song W, Joo M, Yeom J-H, Shin E, Lee M, Choi H-K, Hwang J, Kim Y-I, Seo R, Lee JE, Moore CJ, Kim Y-
471 H, Eyun S-I, Hahn Y, Bae J, Lee K. 2019. Divergent rRNAs as regulators of gene expression at the
472 ribosome level. Nat Microbiol 4:515–526.
- 473 7. Chen Y-X, Xu Z, Ge X, Hong J-Y, Sanyal S, Lu ZJ, Javid B. 2020. Selective translation by alternative
474 bacterial ribosomes. Proc Natl Acad Sci U S A 117:19487–19496.

- 475 8. Sjöstedt A. 2007. Tularemia: History, Epidemiology, Pathogen Physiology, and Clinical
476 Manifestations. *Ann N Y Acad Sci* 1105:1–29.
- 477 9. Barker JR, Chong A, Wehrly TD, Yu J-J, Rodriguez SA, Liu J, Celli J, Arulanandam BP, Klose KE. 2009.
478 The *Francisella tularensis* pathogenicity island encodes a secretion system that is required for
479 phagosome escape and virulence. *Mol Microbiol* 74:1459–1470.
- 480 10. Bröms JE, Meyer L, Sun K, Lavander M, Sjöstedt A. 2012. Unique substrates secreted by the type VI
481 secretion system of *Francisella tularensis* during intramacrophage infection. *PLoS One* 7:e50473.
- 482 11. Eshraghi A, Kim J, Walls AC, Ledvina HE, Miller CN, Ramsey KM, Whitney JC, Radey MC, Peterson SB,
483 Ruhland BR, Tran BQ, Goo YA, Goodlett DR, Dove SL, Celli J, Veessler D, Mougous JD. 2016. Secreted
484 Effectors Encoded within and outside of the Francisella Pathogenicity Island Promote Intramacrophage
485 Growth. *Cell Host Microbe* 20:573–583.
- 486 12. Ledvina HE, Kelly KA, Eshraghi A, Plemel RL, Peterson SB, Lee B, Steele S, Adler M, Kawula TH, Merz
487 AJ, Skerrett SJ, Celli J, Mougous JD. 2018. A Phosphatidylinositol 3-Kinase Effector Alters Phagosomal
488 Maturation to Promote Intracellular Growth of *Francisella*. *Cell Host Microbe* 24:285-295.e8.
- 489 13. Lauriano CM, Barker JR, Yoon S-S, Nano FE, Arulanandam BP, Hassett DJ, Klose KE. 2004. MglA
490 regulates transcription of virulence factors necessary for *Francisella tularensis* intraamoebae and
491 intramacrophage survival. *Proc Natl Acad Sci U S A* 101:4246–4249.

492 14. Charity JC, Costante-Hamm MM, Balon EL, Boyd DH, Rubin EJ, Dove SL. 2007. Twin RNA
493 polymerase-associated proteins control virulence gene expression in *Francisella tularensis*. PLoS
494 Pathog 3:e84.

495 15. Charity JC, Blalock LT, Costante-Hamm MM, Kasper DL, Dove SL. 2009. Small molecule control of
496 virulence gene expression in *Francisella tularensis*. PLoS Pathog 5:e1000641.

497 16. Brotcke A, Monack DM. 2008. Identification of *fevR*, a novel regulator of virulence gene expression
498 in *Francisella novicida*. Infect Immun 76:3473–3480.

499 17. Rohlfing AE, Dove SL. 2014. Coordinate control of virulence gene expression in *Francisella tularensis*
500 involves direct interaction between key regulators. J Bacteriol 196:3516–3526.

501 18. Ramsey KM, Osborne ML, Vvedenskaya IO, Su C, Nickels BE, Dove SL. 2015. Ubiquitous promoter-
502 localization of essential virulence regulators in *Francisella tularensis*. PLoS Pathog 11:e1004793.

503 19. Cuthbert BJ, Ross W, Rohlfing AE, Dove SL, Gourse RL, Brennan RG, Schumacher MA. 2017.
504 Dissection of the molecular circuitry controlling virulence in *Francisella tularensis*. Genes Dev 31:1549–
505 1560.

506 20. Travis BA, Ramsey KM, Prezioso SM, Tallo T, Wandzilak JM, Hsu A, Borgnia M, Bartesaghi A, Dove
507 SL, Brennan RG, Schumacher MA. 2021. Structural Basis for Virulence Activation of *Francisella*
508 *tularensis*. Mol Cell 81:139-152.e10.

509 21. Van Duin J, Wijnands R. 1981. The function of ribosomal protein S21 in protein synthesis. Eur J
510 Biochem 118:615–9.

- 511 22. Chang C, Craven GR. 1977. Identification of several proteins involved in the messenger RNA binding
512 site of the 30 S ribosome by inactivation with 2-methoxy-5-nitrotrypone. J Mol Biol 117:401–18.
- 513 23. Berk V, Zhang W, Pai RD, Cate JHD. 2006. Structural basis for mRNA and tRNA positioning on the
514 ribosome. Proc Natl Acad Sci U S A 103:15830–15834.
- 515 24. Watson ZL, Ward FR, Méheust R, Ad O, Schepartz A, Banfield JF, Cate JH. 2020. Structure of the
516 bacterial ribosome at 2 Å resolution. Elife 9:e60482.
- 517 25. Mizushima S, Nomura M. 1970. Assembly Mapping of 30S Ribosomal Proteins from *E. coli*. Nature
518 226:1214–1218.
- 519 26. Robertson WR, Dowsett SJ, Hardy SJS. 1977. Exchange of ribosomal proteins among the ribosomes
520 of *Escherichia coli*. Mol Gen Genet 157:205–214.
- 521 27. Lupski JR, Godson GN. 1984. The *rpsU-dnaG-rpoD* macromolecular synthesis operon of *E. coli*. Cell
522 39:251–252.
- 523 28. Deniziak M, Sauter C, Becker HD, Paulus CA, Giegé R, Kern D. 2007. Deinococcus glutaminyl-tRNA
524 synthetase is a chimer between proteins from an ancient and the modern pathways of aminoacyl-tRNA
525 formation. Nucleic Acids Res 35:1421–1431.
- 526 29. Searle BC, Swearingen KE, Barnes CA, Schmidt T, Gessulat S, Küster B, Wilhelm M. 2020. Generating
527 high quality libraries for DIA MS with empirically corrected peptide predictions. Nat Commun 11:1548.

- 528 30. Takata R. 1978. Genetic studies of the ribosomal proteins in *Escherichia coli* XI. Mol Gen Genet
529 160:151–155.
- 530 31. Nomura M, Gourse R, Baughman G. 1984. Regulation of the Synthesis of Ribosomes and Ribosomal
531 Components. Annu Rev Biochem 53:75–117.
- 532 32. Nano FE, Zhang N, Cowley SC, Klose KE, Cheung KKM, Roberts MJ, Ludu JS, Letendre GW,
533 Meierovics AI, Stephens G, Elkins KL. 2004. A *Francisella tularensis* Pathogenicity Island Required for
534 Intramacrophage Growth. J Bacteriol 186:6430–6436.
- 535 33. Larsson P, Oyston PCF, Chain P, Chu MC, Duffield M, Fuxelius H-H, Garcia E, Hälltorp G, Johansson
536 D, Isherwood KE, Karp PD, Larsson E, Liu Y, Michell S, Prior J, Prior R, Malfatti S, Sjöstedt A, Svensson K,
537 Thompson N, Vergez L, Wagg JK, Wren BW, Lindler LE, Andersson SGE, Forsman M, Titball RW. 2005.
538 The complete genome sequence of *Francisella tularensis*, the causative agent of tularemia. Nat Genet
539 37:153–159.
- 540 34. Nano FE, Schmerk C. 2007. The *Francisella* Pathogenicity Island. Ann N Y Acad Sci 1105:122–137.
- 541 35. Brotcke A, Weiss DS, Kim CC, Chain P, Malfatti S, Garcia E, Monack DM. 2006. Identification of
542 MglA-regulated genes reveals novel virulence factors in *Francisella tularensis*. Infect Immun 74:6642–
543 6655.
- 544 36. Yutin N, Puigbo P, Koonin EV, Wolf YI. 2012. Phylogenomics of prokaryotic ribosomal proteins. PLoS
545 One 7:e36972.

546 37. Galperin MY, Wolf YI, Garushyants SK, Alvarez RV, Koonin EV. 2021. Nonessential Ribosomal
547 Proteins in Bacteria and Archaea Identified Using Clusters of Orthologous Genes. J Bacteriol
548 203:e00058.

549 38. Bubunenko M, Baker T, Court DL. 2007. Essentiality of ribosomal and transcription antitermination
550 proteins analyzed by systematic gene replacement in *Escherichia coli*. J Bacteriol 189:2844–2853.

551 39. Yamamoto N, Nakahigashi K, Nakamichi T, Yoshino M, Takai Y, Touda Y, Furubayashi A, Kinjyo S,
552 Dose H, Hasegawa M, Datsenko KA, Nakayashiki T, Tomita M, Wanner BL, Mori H. 2009. Update on the
553 Keio collection of *Escherichia coli* single-gene deletion mutants. Mol Syst Biol 5:335.

554 40. Goodall ECA, Robinson A, Johnston IG, Jabbari S, Turner KA, Cunningham AF, Lund PA, Cole JA,
555 Henderson IR. 2018. The Essential Genome of *Escherichia coli* K-12. mBio 9:e02096-17.

556 41. Ramsey KM, Ledvina HE, Tresko TM, Wandzilak JM, Tower CA, Tallo T, Schramm CE, Peterson SB,
557 Skerrett SJ, Mougous JD, Dove SL. 2020. Tn-Seq reveals hidden complexity in the utilization of host-
558 derived glutathione in *Francisella tularensis*. PLoS Pathog 16:e1008566.

559 42. Jha V, Roy B, Jahagirdar D, McNutt ZA, Shatoff EA, Boleratz BL, Watkins DE, Bundschuh R, Basu K,
560 Ortega J, Fredrick K. 2020. Structural basis of sequestration of the anti-Shine-Dalgarno sequence in the
561 Bacteroidetes ribosome. Nucleic Acids Res 49:547–567.

562 43. Takada H, Morita M, Shiwa Y, Sugimoto R, Suzuki S, Kawamura F, Yoshikawa H. 2014. Cell motility
563 and biofilm formation in *Bacillus subtilis* are affected by the ribosomal proteins, S11 and S21. Biosci
564 Biotechnol Biochem 78:898–907.

- 565 44. Metselaar KI, Besten HMW den, Boekhorst J, Hijum SAFT van, Zwietering MH, Abee T. 2015.
566 Diversity of acid stress resistant variants of *Listeria monocytogenes* and the potential role of ribosomal
567 protein S21 encoded by *rpsU*. Front Microbiol 6:422.
- 568 45. Metselaar KI, Abee T, Zwietering MH, Besten HMW den. 2016. Modeling and Validation of the
569 Ecological Behavior of Wild-Type *Listeria monocytogenes* and Stress-Resistant Variants. Appl Environ
570 Microbiol 82:5389–5401.
- 571 46. Basco MDS, Kothari A, McKinzie PB, Revollo JR, Agnihothram S, Azevedo MP, Saccente M, Hart ME.
572 2019. Reduced vancomycin susceptibility and increased macrophage survival in *Staphylococcus aureus*
573 strains sequentially isolated from a bacteraemic patient during a short course of antibiotic therapy. J
574 Med Microbiol 68:848–859.
- 575 47. Blake KL, O'Neill AJ. 2013. Transposon library screening for identification of genetic loci
576 participating in intrinsic susceptibility and acquired resistance to antistaphylococcal agents. J
577 Antimicrob Chemother 68:12–16.
- 578 48. Friedman L, Alder JD, Silverman JA. 2006. Genetic Changes That Correlate with Reduced
579 Susceptibility to Daptomycin in *Staphylococcus aureus*. Antimicrob Agents Chemother 50:2137–2145.
- 580 49. Gutierrez MG, Yoder-Himes DR, Warawa JM. 2015. Comprehensive identification of virulence
581 factors required for respiratory melioidosis using Tn-seq mutagenesis. Front Cell Infect Microbiol 5:78.
- 582 50. Su J, Yang J, Zhao D, Kawula TH, Banas JA, Zhang J-R. 2007. Genome-Wide Identification of
583 *Francisella tularensis* Virulence Determinants. Infect Immun 75:3089–3101.

584 51. Mizuno CM, Guyomar C, Roux S, Lavigne R, Rodriguez-Valera F, Sullivan MB, Gillet R, Forterre P,
585 Krupovic M. 2019. Numerous cultivated and uncultivated viruses encode ribosomal proteins. Nat
586 Commun 10:752.

587 52. Al-Shayeb B, Sachdeva R, Chen L-X, Ward F, Munk P, Devoto A, Castelle CJ, Olm MR, Bouma-
588 Gregson K, Amano Y, He C, Méheust R, Brooks B, Thomas A, Lavy A, Matheus-Carnevali P, Sun C,
589 Goltsman DSA, Borton MA, Sharrar A, Jaffe AL, Nelson TC, Kantor R, Keren R, Lane KR, Farag IF, Lei S,
590 Finstad K, Amundson R, Anantharaman K, Zhou J, Probst AJ, Power ME, Tringe SG, Li W-J, Wrighton K,
591 Harrison S, Morowitz M, Relman DA, Doudna JA, Lehours A-C, Warren L, Cate JHD, Santini JM, Banfield
592 JF. 2020. Clades of huge phages from across Earth’s ecosystems. Nature 578:425–431.

593 53. Chen L-X, Jaffe AL, Borges AL, Penev PI, Nelson TC, Warren LA, Banfield JF. 2022. Phage-encoded
594 ribosomal protein S21 expression is linked to late-stage phage replication. ISME Commun 2:31.

595 54. Maier TM, Havig A, Casey M, Nano FE, Frank DW, Zahrt TC. 2004. Construction and Characterization
596 of a Highly Efficient *Francisella* Shuttle Plasmid. Appl Environ Microbiol 70:7511–7519.

597 55. Ramsey KM, Dove SL. 2016. A response regulator promotes *Francisella tularensis* intramacrophage
598 growth by repressing an anti-virulence factor. Mol Microbiol 101:688–700.

599 56. Skeggs PA, Thompson J, Cundliffe E. 1985. Methylation of 16S ribosomal RNA and resistance to
600 aminoglycoside antibiotics in clones of *Streptomyces lividans* carrying DNA from *Streptomyces*
601 *tenjimariensis*. Mol Gen Genet 200:415–421.

602 57. Johnson GE, Li G-W. 2018. Genome-Wide Quantitation of Protein Synthesis Rates in Bacteria.
603 Methods Enzymol 612:225–249.

604

605 **FIGURES**

606

607 **Figure 1. *F. tularensis* ribosomes are heterogenous with respect to bS21.** **A.** Chart demonstrating
608 purity of wild-type ribosomes. Categories represent classification of proteins identified by mass
609 spectrometry of ribosomes purified from wild-type *F. tularensis* LVS cells. Numbers represent the
610 percentage of spectral counts corresponding to proteins in each category, combined from
611 quadruplicate samples. **B.** Wild-type *F. tularensis* LVS ribosomes contain more than one bS21 homolog.
612 Table detailing the number of spectral counts corresponding to bS21 homologs identified from
613 individual ribosome purifications (A – D) from wild-type cells. Spectral counts corresponding to bS21-1
614 and/or bS21-3 cannot be unambiguously assigned due to complete sequence identity of detected
615 peptides. ND: not detected. **C.** Each bS21 homolog can be incorporated into ribosomes. Top: Sucrose
616 gradient sedimentation profile from actively-translating wild-type cells containing an empty vector.
617 Nucleic acid content was monitored by A260 (y-axis). Peaks corresponding to the 30S, 50S, 70S, and
618 polysomes are indicated. Fractions collected are indicated on the x-axis. Bottom: Immunoblot analysis
619 of fractions from sucrose gradient sedimentation performed on actively-translating cells ectopically
620 expressing indicated bS21 homolog with VSV-G epitope tag. Wells correspond to fractions 1 – 21 from
621 profile above.

622

623 **Figure 2. Loss of bS21-2 leads to changes in protein abundance that cannot be explained by changes**
624 **in transcript abundance.** Cells with (WT, wild-type) and without bS21-2 ($\Delta rpsU2$) were analyzed using
625 RNA-Seq (x-axis) and DIA whole cell mass spectrometry (y-axis). Genes are represented by dots. Most
626 genes with changes in protein (161 yellow dots) do not have corresponding changes in transcript
627 abundance. One gene (orange dot) has discordant changes in transcript and protein abundance. Green

dots (23) represent genes with concordant changes in transcript and protein abundance. Blue dots (60) indicate genes with altered transcript abundance only. Horizontal dashed lines indicate +/- 1.5-fold cutoff for differential protein abundance; vertical dashes indicate +/- 2-fold cutoff for differential transcript abundance. Colored dots with black outlines represent genes with significant changes in protein (+/- 1.5-fold change, adjusted p-value <0.05) and/or transcript (+/- 2-fold change, adjusted p-value <0.05) abundance as indicated above, while grey dots without outline represent genes with changes that did not meet the statistical thresholds. Three grey dots are located outside the bounds of the axis as represented.

Figure 3. bS21-2 is a regulator of T6SS protein abundance. A. Immunoblot analysis of indicated T6SS protein abundance. As indicated, cells either contained (wild-type) or lacked ($\Delta rpsU2$) bS21-2 and either an empty vector control (pF) or a vector ectopically expressing VSV-G-tagged bS21-2 (pF-bS21-2-V). Immunoblot against VSV-G was included to demonstrate production of VSV-G-tagged bS21 homologs. **B.** Quantification of immunoblots from (A). Band intensities for each protein were normalized to total protein per well on the membrane. Error bars represent 1 SD. Experiments were repeated at least twice and data from a representative experiment are shown. Lines above bars indicate statistical comparison among groups by t-test. Asterisk indicates group to which all other groups are compared, if horizontal line connects to line above group, $*p < 0.05$ using Benjamini-Hochberg correction.

Figure 4. Cells without bS21-2 have an intramacrophage growth defect, which can be complemented by ectopic expression of bS21-2. Growth and survival of *F. tularensis* LVS cells within J774A.1 cells.

650 Murine macrophage-like J774A.1 cells were infected with indicated bacterial cells at a multiplicity of
651 infection of 5 – 10. J774A.1 cells were lysed and bacteria were plated for enumeration (colony forming
652 units [CFU]) at 2 and 24 hours post-infection. Error bars represent 1 SD. Experiments were repeated at
653 least twice and data from a representative experiment are shown. Lines above bars indicate statistical
654 comparison among groups by t-test. Asterisk indicates group to which all other groups are compared, if
655 horizontal line connects to line above group, $*p < 0.05$ using Benjamini-Hochberg correction.

656

657 SUPPLEMENTAL MATERIAL

658

659 SUPPLEMENTAL FIGURES

660

661 **Figure S1. *F. tularensis* encodes three *rpsU* genes.** *F. tularensis rpsU2*, which encodes bS21-2, is
662 syntenic with the only *rpsU* in *E. coli*, which is located in the macromolecular synthesis operon (1). This
663 operon in *E. coli* includes *rpsU* (encoding bS21), *dnaG* (encoding DNA primase), and *rpoD* (encoding
664 RNA polymerase σ^{70}). In *F. tularensis*, this operon also includes *yqeY*, the product of which may be
665 involved in tRNA aminoacylation. *rpsU1*, encoding bS21-1, is located immediately downstream of *cspC*
666 (encoding cold-shock protein CspC), while *rpsU3*, encoding bS21-3, is not apparently in an operon with
667 other genes. Genomic locations of *rpsU* genes were determined using RefSeq NC_007880 for *F.*
668 *tularensis* and NC_000913 for *E. coli*.

669

670 **Figure S2. The three bS21 homologs in *F. tularensis* are distinct.** Percent identities of amino acid
671 sequences for *F. tularensis* LVS bS21-1, bS21-2, bS21-3 and *E. coli* bS21 were calculated using the

multiple sequence alignment tool ClustalOmega (2). The bS21 homologs in *F. tularensis* are similar to each other, particularly bS21-1 and bS21-3 which are 72% identical at the amino acid level. bS21-2, encoded by the *rpsU* homolog gene syntenic to the single *E. coli rpsU* gene, is also the most similar to *E. coli* bS21, with 60% amino acid identity.

Figure S3. Each bS21 homolog can be detected in translationally-active ribosomes. For **A – D**, top: Sucrose gradient sedimentation profile from actively-translating wild-type *F. tularensis* cells with either empty vector or ectopic expression of indicated bS21 homolog. Nucleic acid content was monitored by A260 (y-axis). Peaks corresponding to the 30S, 50S, 70S, and polysomes are indicated. Fractions collected are indicated on the x-axis. For **A – D**, bottom: Immunoblot analysis of fractions from sucrose gradient sedimentation (above), probing for VSV-G. Wells correspond to fractions 1 – 21 from profile above. **A.** Cells from wild-type *F. tularensis* LVS with empty vector (LVS pF). **B.** Cells from wild-type *F. tularensis* LVS with ectopic expression of bS21-1 (LVS pF-bS21-1-V). **C.** Cells from wild-type *F. tularensis* LVS with ectopic expression of bS21-2 (LVS pF-bS21-2-V). **D.** Cells from wild-type *F. tularensis* LVS with ectopic expression of bS21-3 (LVS pF-bS21-3-V).

Figure S4. Loss of bS21-2 does not affect transcript abundance of FPI-encoded genes. Quantitative real-time PCR was used to determine the relative transcript abundance for indicated FPI genes in wild-type cells, cells lacking bS21-2 ($\Delta rpsU2$), or cells lacking the transcription factor PigR ($\Delta pigR$). Cells lacking PigR serve as a positive control, as PigR positively regulates its own transcription and the transcription of *pdpA*, *pdpB*, and *iglA*. The *rpoA1* and *bfr* genes are included as negative controls, as their expression is not influenced by bS21-2 or PigR. Transcript abundances are normalized to *tul4*,

694 whose expression is not influenced by bS21-2 or PigR. Error bars represent 1 SD from the value
695 (calculated using the mean threshold cycle). ns: not significant. ND: not detected *adjusted $p < 0.05$ by
696 t-test.

697

698 **Figure S5. Loss of bS21-2 does not affect protein degradation of PdpB.** One-phase decay of PdpB from
699 antibiotic-chase experiment from wild-type cells and cells lacking bS21-2 ($\Delta rpsU2$). Neither strain
700 showed significant degradation of PdpB through the time points assessed; the calculated half-life for
701 both was greater than 120 minutes. Y-axis is logarithmic and error bars represent 1 standard deviation
702 from the mean.

703

704 **SUPPLEMENTAL TABLES**

705

706 **Table S1. Proteins associated with purified *F. tularensis* ribosomes.** LC-MS/MS analysis of four
707 samples of ribosomes purified from wild-type cells by sucrose cushions. Total spectral counts (columns
708 F-I) were filtered with the following parameters: 99% protein threshold, 95% peptide threshold,
709 minimum of 2 peptides. Hypothetical proteins with no known function were not categorized as
710 transcription or translation-related. Proteins were primarily ribosomal (69%) or associated with
711 transcription and translation processes (10%).

712

713 **Table S2. Cells lacking bS21-2 exhibit genome-wide changes in protein abundance.** Data-independent
714 acquisition (DIA) mass spectrometry analysis of cellular lysates was used to quantify genome-wide
715 protein abundance in wild-type cells (WT), cells lacking bS21-1 ($\Delta rpsU1$), cells lacking bS21-2

(delt_rpsU2), and cells lacking bS21-3 (delt_rpsU3). Each deletion strain was compared to wild-type, but significant changes (>1.5-fold change, adjusted p-value <0.05, excluding bS21) were only observed in the cells lacking bS21-2. Cells are highlighted if the fold-change (columns R, U, and X) is greater than 1.5 ($\log_2FC > 0.58$ or < -0.58). Green indicates less abundant in deletion strains compared to wild-type, and red indicates more abundant. Adjusted p-values are highlighted red if <0.05 (columns T, W, and Z).

721

Table S3. Cells lacking bS21-2 have significant changes in transcript abundance. RNA-Seq was used to compare genome-wide transcript abundance from wild-type cells with an empty vector (LVS pF), cells lacking bS21-2 and containing an empty vector (LVS $\Delta rpsU2$ pF), and bS21-2 mutant cells with bS21-2-V ectopically expressed (LVS $\Delta rpsU2$ pF-*rpsU2*-V). Transcripts with significant differences in cells lacking bS21-2 compared to wild-type (>2-fold change, adjusted p-value <0.05) are included (columns E-F). All changes were complemented by ectopic expression of bS21-2-V (columns G-J). Base mean (column D) reflects a measure of transcript abundance across all strains.

729

Table S4. RNA-Seq reveals that cells without bS21-2 do not have transcript reductions across the Francisella Pathogenicity Island. Of the 16 Francisella Pathogenicity Island (FPI) genes encoded by *F. tularensis* LVS, only two genes are significantly differentially expressed at the transcript level in cells lacking bS21-2 compared to wild-type ($\log_2FC > 1.00$ or < -1.00 , adjusted p-value <0.05). These changes are complemented by ectopic expression of bS21-2-V on a plasmid.

735

Table S5. Comparison of *in vitro* and intramacrophage growth rates for strains used in this study. *In vitro* growth was assessed during early exponential phase by measuring OD₆₀₀. *In vitro* generation

737

738 times for LVS pF, LVS *ΔrpsU2* pF, and LVS *ΔrpsU2* pF-bS21-2-V were calculated from three independent
739 experiments, others were calculated from two. Generation times for intramacrophage growth are
740 averages across three independent experiments and were determined by comparison of CFU
741 recovered after 2 versus 24 hours. +/- values indicate SD.

742

743 **Supplemental References**

744

745 1. Lupski JR, Godson GN. 1984. The *rpsU-dnaG-rpoD* macromolecular synthesis operon of *E. coli*. Cell
746 39:251–252.

747 2. Madeira F, Pearce M, Tivey ARN, Basutkar P, Lee J, Edbali O, Madhusoodanan N, Kolesnikov A, Lopez
748 R. 2022. Search and sequence analysis tools services from EMBL-EBI in 2022. Nucleic Acids Res
749 50:W276–W279.

750

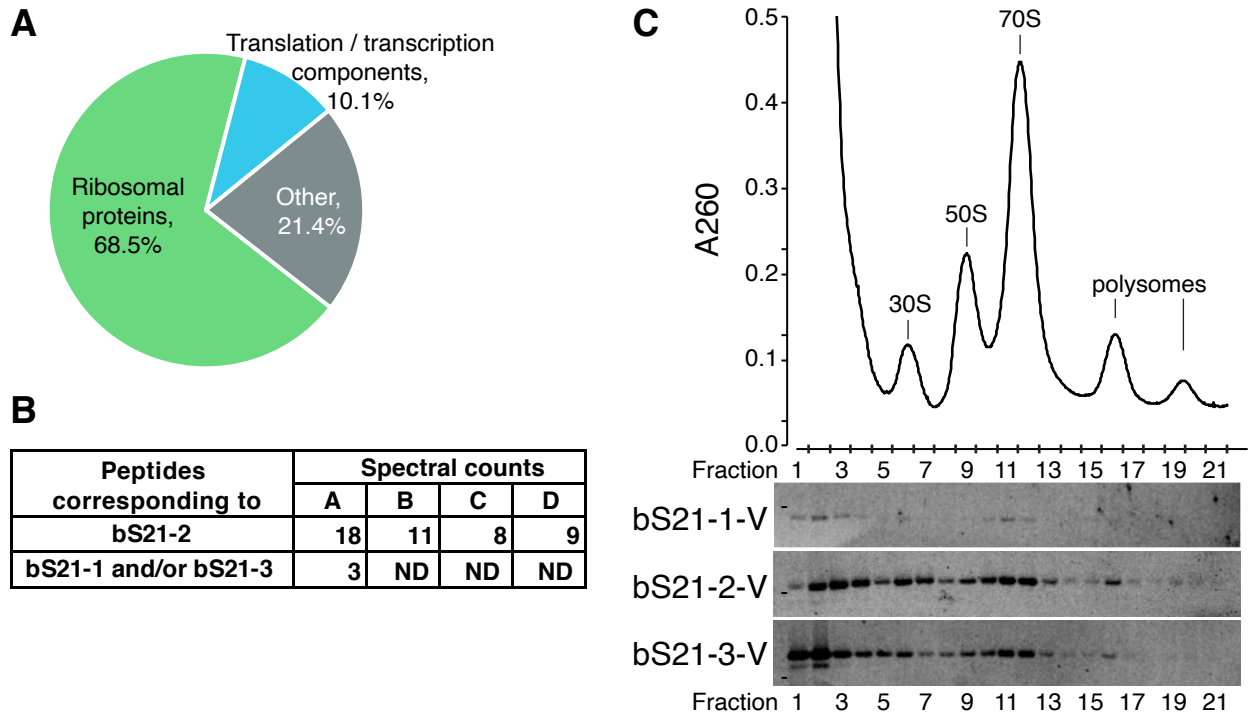


Figure 1. *F. tularensis* ribosomes are heterogenous with respect to bS21. **A.** Chart demonstrating purity of wild-type ribosomes. Categories represent classification of proteins identified by mass spectrometry of ribosomes purified from wild-type *F. tularensis* LVS cells. Numbers represent the percentage of spectral counts corresponding to proteins in each category, combined from quadruplicate samples. **B.** Wild-type *F. tularensis* LVS ribosomes contain more than one bS21 homolog. Table detailing the number of spectral counts corresponding to bS21 homologs identified from individual ribosome purifications (A – D) from wild-type cells. Spectral counts corresponding to bS21-1 and/or bS21-3 cannot be unambiguously assigned due to complete sequence identity of detected peptides. ND: not detected. **C.** Each bS21 homolog can be incorporated into ribosomes. Top: Sucrose gradient sedimentation profile from actively-translating wild-type cells containing an empty vector. Nucleic acid content was monitored by A260 (y-axis). Peaks corresponding to the 30S, 50S, 70S, and polysomes are indicated. Fractions collected are indicated on the x-axis. Bottom: Immunoblot analysis of fractions from sucrose gradient sedimentation performed on actively-translating cells ectopically expressing indicated bS21 homolog with VSV-G epitope tag. Wells correspond to fractions 1 – 21 from profile above.

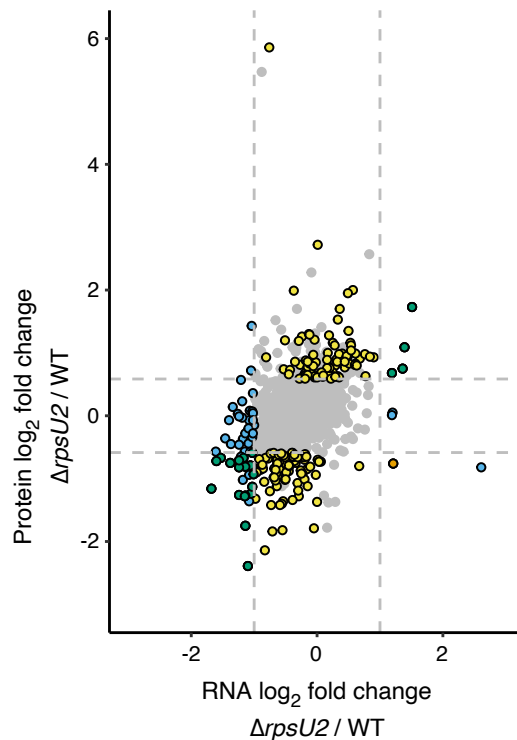


Figure 2. Loss of bS21-2 leads to changes in protein abundance that cannot be explained by changes in transcript abundance. Cells with (WT, wild-type) and without bS21-2 ($\Delta rpsU2$) were analyzed using RNA-Seq (x-axis) and DIA whole cell mass spectrometry (y-axis). Genes are represented by dots. Most genes with changes in protein (161 yellow dots) do not have corresponding changes in transcript abundance. One gene (orange dot) has discordant changes in transcript and protein abundance. Green dots (23) represent genes with concordant changes in transcript and protein abundance. Blue dots (60) indicate genes with altered transcript abundance only. Horizontal dashed lines indicate +/- 1.5-fold cutoff for differential protein abundance; vertical dashes indicate +/- 2-fold cutoff for differential transcript abundance. Colored dots with black outlines represent genes with significant changes in protein (+/- 1.5-fold change, adjusted p-value <0.05) and/or transcript (+/- 2-fold change, adjusted p-value <0.05) abundance as indicated above, while grey dots without outline represent genes with changes that did not meet the statistical thresholds. Three grey dots are located outside the bounds of the axis as represented.

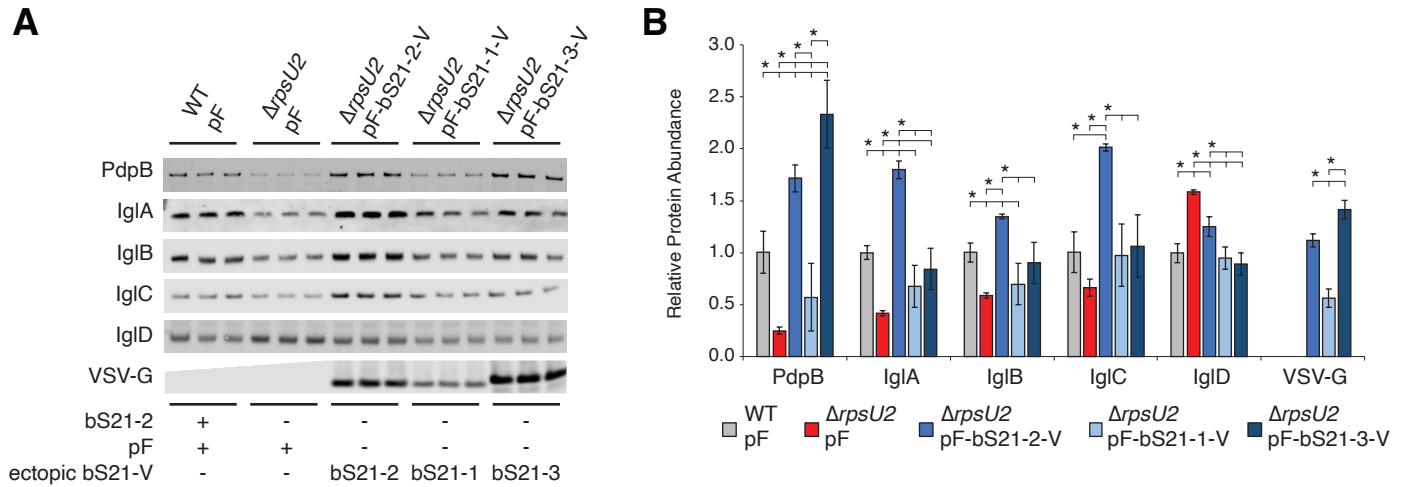


Figure 3. bS21-2 is a regulator of T6SS protein abundance. A. Immunoblot analysis of indicated T6SS protein abundance. As indicated, cells either contained (wild-type) or lacked ($\Delta rpsU2$) bS21-2 and either an empty vector control (pF) or a vector ectopically expressing VSV-G-tagged bS21-2 (pF-bS21-2-V). Immunoblot against VSV-G was included to demonstrate production of VSV-G-tagged bS21 homologs. **B.** Quantification of immunoblots from (A). Band intensities for each protein were normalized to total protein per well on the membrane. Error bars represent 1 SD. Experiments were repeated at least twice and data from a representative experiment are shown. Lines above bars indicate statistical comparison among groups by t-test. Asterisk indicates group to which all other groups are compared, if horizontal line connects to line above group, * $p < 0.05$ using Benjamini-Hochberg correction.

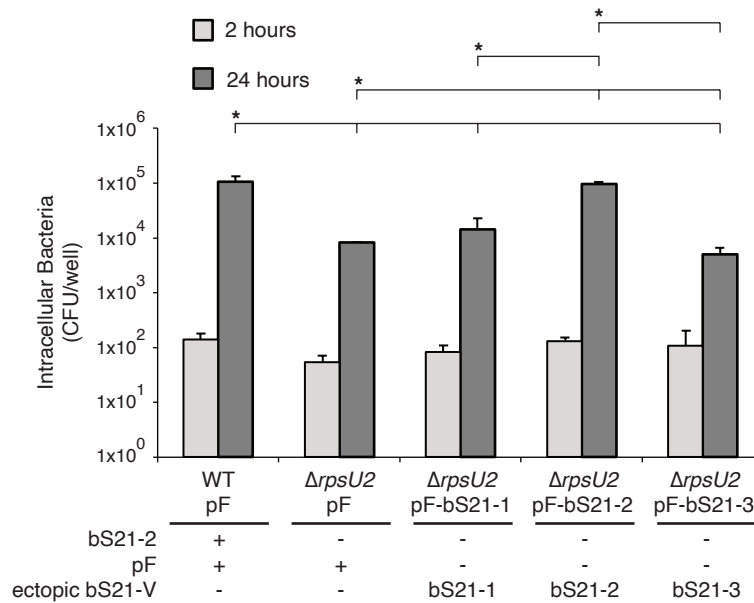
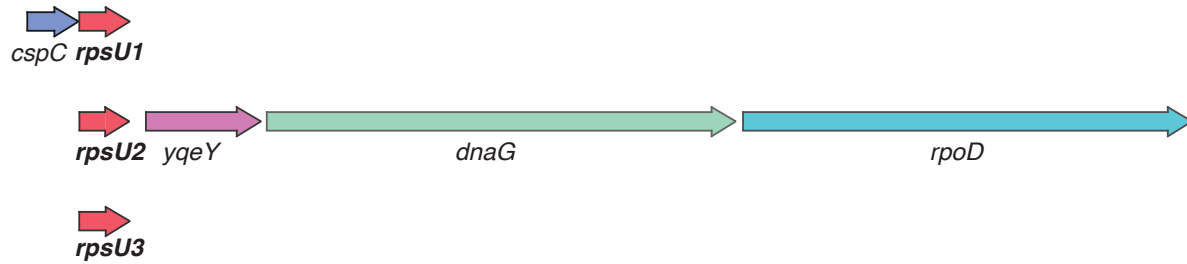


Figure 4. Cells without bS21-2 have an intramacrophage growth defect, which can be complemented by ectopic expression of bS21-2. Growth and survival of *F. tularensis* LVS cells within J774A.1 cells. Murine macrophage-like J774A.1 cells were infected with indicated bacterial cells at a multiplicity of infection of 5 – 10. J774A.1 cells were lysed and bacteria were plated for enumeration (colony forming units [CFU]) at 2 and 24 hours post-infection. Error bars represent 1 SD. Error bars for the LVS $\Delta rpsU2$ cells at the 24 hour time point are too small to be illustrated. Experiments were repeated at least twice and data from a representative experiment are shown. Lines above bars indicate statistical comparison among groups by t-test. Asterisk indicates group to which all other groups are compared, if horizontal line connects to line above group, * $p < 0.05$ using Benjamini-Hochberg correction.

Francisella tularensis



Escherichia coli



Figure S1. *F. tularensis* encodes three *rpsU* genes. *F. tularensis* *rpsU2*, which encodes bS21-2, is syntenic with the only *rpsU* in *E. coli*, which is located in the macromolecular synthesis operon (1). This operon in *E. coli* includes *rpsU* (encoding bS21), *dnaG* (encoding DNA primase), and *rpoD* (encoding RNA polymerase σ^{70}). In *F. tularensis*, this operon also includes *yqeY*, the product of which may be involved in tRNA aminoacylation. *rpsU1*, encoding bS21-1, is located immediately downstream of *cspC* (encoding cold-shock protein CspC), while *rpsU3*, encoding bS21-3, is not apparently in an operon with other genes. Genomic locations of *rpsU* genes were determined using RefSeq NC_007880 for *F. tularensis* and NC_000913 for *E. coli*.

	<i>F. tularensis</i> subsp <i>holarctica</i> LVS bS21-1	<i>F. tularensis</i> subsp <i>holarctica</i> LVS bS21-3	<i>F. tularensis</i> subsp <i>holarctica</i> LVS bS21-2	<i>E. coli</i> bS21
<i>F. tularensis</i> subsp <i>holarctica</i> LVS bS21-1	100.0	72.3	54.0	50.8
<i>F. tularensis</i> subsp <i>holarctica</i> LVS bS21-3		100.0	47.6	48.5
<i>F. tularensis</i> subsp <i>holarctica</i> LVS bS21-2			100.0	60.0
<i>E. coli</i> bS21				100.0

Figure S2. The three bS21 homologs in *F. tularensis* are distinct. Percent identities of amino acid sequences for *F. tularensis* LVS bS21-1, bS21-2, bS21-3, and *E. coli* bS21 were calculated using the multiple sequence alignment tool ClustalOmega (2). The bS21 homologs in *F. tularensis* are similar to each other, particularly bS21-1 and bS21-3 which are 72% identical at the amino acid level. bS21-2, encoded by the *rpsU* homolog gene syntenic to the single *E. coli* *rpsU* gene, is also the most similar to *E. coli* bS21, with 60% amino acid identity.

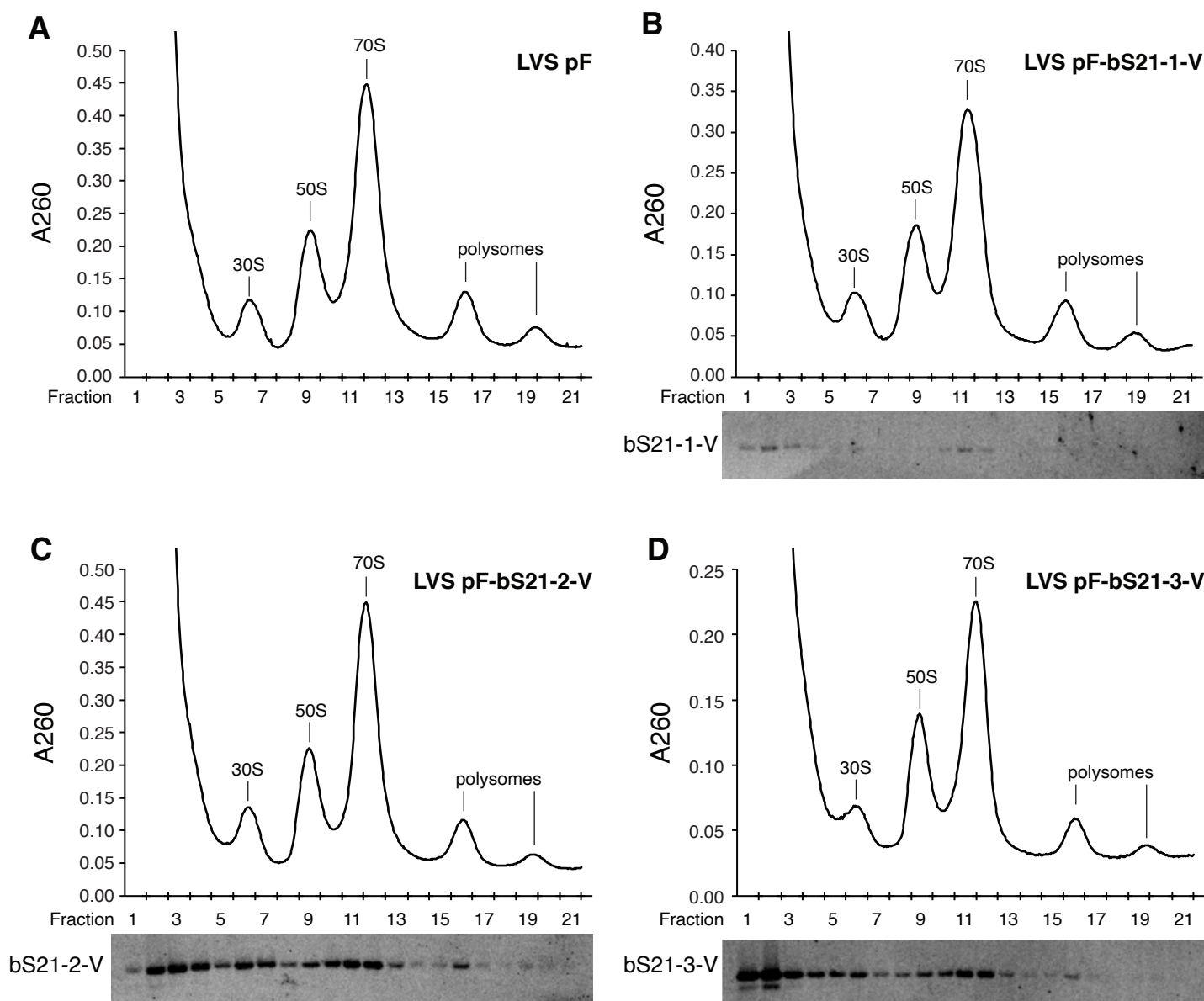


Figure S3. Each bS21 homolog can be detected in translationally-active ribosomes. For **A – D**, top: Sucrose gradient sedimentation profile from actively-translating wild-type *F. tularensis* cells with either empty vector or ectopic expression of indicated bS21 homolog. Nucleic acid content was monitored by A260 (y-axis). Peaks corresponding to the 30S, 50S, 70S, and polysomes are indicated. Fractions collected are indicated on the x-axis. For **A – D**, bottom: Immunoblot analysis of fractions from sucrose gradient sedimentation (above), probing for VSV-G. Wells correspond to fractions 1 – 21 from profile above. **A.** Cells from wild-type *F. tularensis* LVS with empty vector (LVS pF). **B.** Cells from wild-type *F. tularensis* LVS with ectopic expression of bS21-1 (LVS pF-bS21-1-V). **C.** Cells from wild-type *F. tularensis* LVS with ectopic expression of bS21-2 (LVS pF-bS21-2-V). **D.** Cells from wild-type *F. tularensis* LVS with ectopic expression of bS21-3 (LVS pF-bS21-3-V).

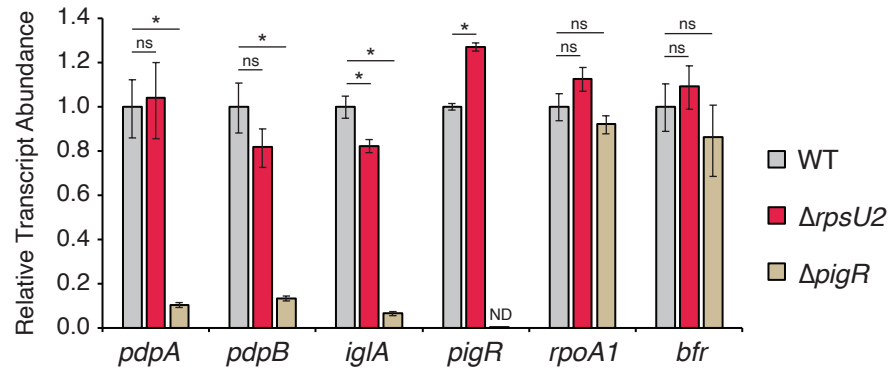


Figure S4. Loss of bS21-2 does not affect transcript abundance of FPI-encoded genes.

Quantitative real-time PCR was used to determine the relative transcript abundance for indicated FPI genes in wild-type cells, cells lacking bS21-2 ($\Delta rpsU2$), or cells lacking the transcription factor PigR ($\Delta pigR$). Cells lacking PigR serve as a positive control, as PigR positively regulates its own transcription and the transcription of *pdpA*, *pdpB*, and *iglA*. The *rpoA1* and *bfr* genes are included as negative controls, as their expression is not influenced by bS21-2 or PigR. Transcript abundances are normalized to *tul4*, whose expression is not influenced by bS21-2 or PigR. Error bars represent 1 SD from the value (calculated using the mean threshold cycle). ns: not significant. ND: not detected. *adjusted $p < 0.05$ by t-test.

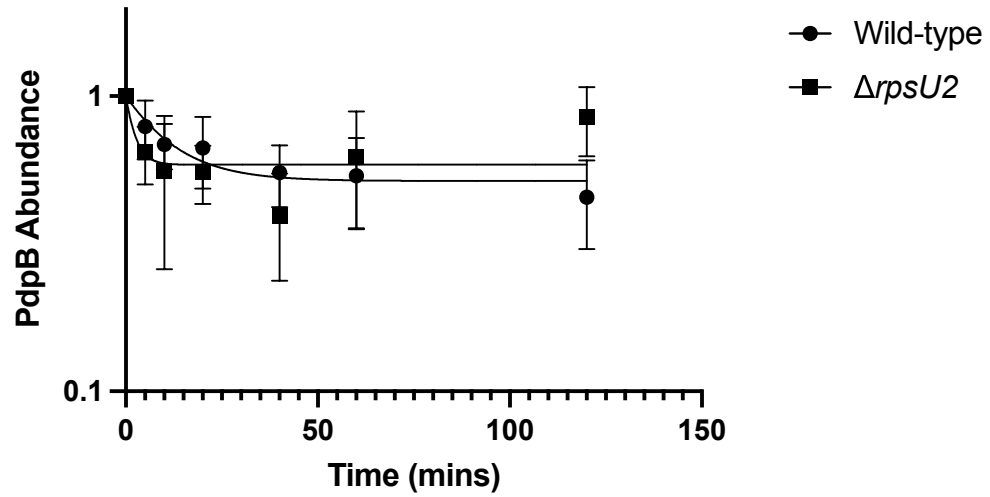


Figure S5. Loss of bS21-2 does not affect protein degradation of PdpB. One-phase decay of PdpB from antibiotic-chase experiment from wild-type cells and cells lacking bS21-2 ($\Delta rpsU2$). Neither strain showed significant degradation of PdpB through the time points assessed; the calculated half-life for both was greater than 120 minutes. Y-axis is logarithmic and error bars represent 1 SD from the mean.